REPORT

Mutations Impairing GSK3-Mediated MAF Phosphorylation Cause Cataract, Deafness, Intellectual Disability, Seizures, and a Down Syndrome-like Facies

Marcello Niceta,[1,2,22] Emilia Stellacci,[1,22] Karen W. Gripp,[3,23] Giuseppe Zampino,[4,23] Maria Kousi,[5] Massimiliano Anselmi,[6] Alice Traversa,[1,7] Andrea Ciolfi,[1] Deborah Stabley,[8] Alessandro Bruselles,[1] Viviana Caputo,[7] Serena Cecchetti,[9] Sabrina Prudente,[10] Maria T. Fiorenza,[11] Carla Boitani,[12] Nicole Philip,[13] Dmitriy Niyazov,[14] Chiara Leoni,[4] Takaya Nakane,[15] Kim Keppler-Noreuil,[16] Stephen R. Braddock,[17] Gabriele Gillessen-Kaesbach,[18] Antonio Palleschi,[6] Philippe M. Campeau,[19] Brendan H.L. Lee,[20] Celio Pouponnot,[21] Lorenzo Stella,[6] Gianfranco Bocchinfuso,[6] Nicholas Katsanis,[5] Katia Sol-Church,[8] and Marco Tartaglia[1,2,*]

Transcription factors operate in developmental processes to mediate inductive events and cell competence, and perturbation of their function or regulation can dramatically affect morphogenesis, organogenesis, and growth. We report that a narrow spectrum of amino-acid substitutions within the transactivation domain of the v-maf avian musculoaponeurotic fibrosarcoma oncogene homolog (MAF), a leucine zipper-containing transcription factor of the AP1 superfamily, profoundly affect development. Seven different de novo missense mutations involving conserved residues of the four GSK3 phosphorylation motifs were identified in eight unrelated individuals. The distinctive clinical phenotype, for which we propose the eponym Aymé-Gripp syndrome, is not limited to lens and eye defects as previously reported for MAF/Maf loss of function but includes sensorineural deafness, intellectual disability, seizures, brachycephaly, distinctive flat facial appearance, skeletal anomalies, mammary gland hypoplasia, and reduced growth. Disease-causing mutations were demonstrated to impair proper MAF phosphorylation, ubiquitination and proteasomal degradation, perturbed gene expression in primary skin fibroblasts, and induced neurodevelopmental defects in an in vivo model. Our findings nosologically and clinically delineate a previously poorly understood recognizable multisystem disorder, provide evidence for MAF governing a wider range of developmental programs than previously appreciated, and describe a novel instance of protein dosage effect severely perturbing development.

Dual sensory impairment due to cataracts and sensorineural hearing loss is a well-recognized consequence of infectious teratogenic exposure (i.e., fetal rubella syndrome), but only rarely observed as a developmental defect in genetic disease phenotypes. In 1996, Gripp and co-workers described two unrelated subjects with congenital cataracts and sensorineural deafness associated with intellectual disability, short stature, brachycephaly, and a distinctive flat facial appearance and considered this trait to represent a previously unrecognized syndrome (MIM 601088).[1] In their clinical report,[2] Aymé and Philip discussed on the similarities between the clinical features exhibited by their case and others previously reported by other authors[4] and those of the patients reported by Gripp and co-authors.[1] Aymè and Philip concluded that all these cases were clinically related to the patient originally described by Fine and Lubinsky.[3] For this reason, the authors proposed the term "Fine-Lubinsky syndrome" to define this developmental disorder. Since then, a few additional cases exhibiting features fitting or partially overlapping this condition(s) have been reported,[5–9] and whether these phenotypes represent variable manifestations of a single nosologic entity remained unresolved. Autosomal recessive inheritance was suggested, based on affected siblings.[7] Here, whole-exome sequencing (WES) on a single affected individual and Sanger sequencing on a selected cohort of subjects

with phenotype suggestive of FLS were used to identify a narrow spectrum of missense mutations in v-maf avian musculoaponeurotic fibrosarcoma oncogene homolog (*MAF* [MIM 177075]) as the molecular cause underlying this previously poorly understood multisystem disorder, and delineate its clinical phenotype. The provided biochemical and functional data demonstrate that the mutations identified in this study specifically affect the phosphorylation of MAF promoted by the protein GSK3, which is a serine/threonine kinase that requires a specific recognition motif for its action—i.e., the presence of a proline residue adjacent to the serine/threonine residue that is substrate of its action. The impaired phosphorylation at those sites affects MAF ubiquitination, which, in turn, impairs degradation of the mutated (unphosphorylated and unubiquitinilated) protein, generally mediated by the proteasome complex. Finally, these mutations are able to induce neurodevelopmental defects in vivo (zebrafish), thus representing dominant-acting mutations.

Thirteen subjects were included in this study. All individuals were clinically assessed by experienced clinical geneticists. Among them, nine subjects had previously been reported.[1,2,5–8] Clinical features are described in detail in Table S1. Clinical data and biological material collection and storage were attained from the participating families after written informed consent was secured, following procedures in accordance with the ethical standards of the responsible committees on human experimentation (institutional and national). Genomic DNA was isolated from peripheral blood leukocytes, skin fibroblasts, hair bulb cells, and/or buccal mucosal epithelial cells, using standard protocols. We performed WES on genomic DNA extracted from circulating leukocytes of a single affected subject (case 8) (Figure 1A, CaGi_UCSC). Exome capture was performed using NimbleGen SeqCap EZ Exome V. 3.0 (Roche) and sequencing by a HiSeq2000 instrument (Illumina). WES data analysis was performed using an in-house implemented pipeline.[10] For sequencing statistics, see Table S2. Data annotation predicted 11,168 high-quality variants having functional impact (i.e., nonsynonymous and splice site changes). Among them, 259 private, rare (minor allele frequency < 0.001), or clinically associated changes were retained for further analyses. After excluding the presence of variants compatible with autosomal recessive transmission (Table S3), we reasoned that the clinical symptomatology might be caused by a de novo event. Candidates were stratified through a mixed filtering/prioritization strategy taking into account the predicted impact of each variant and the functional relevance of individual genes on the developmental processes altered in the disorder. Only changes (private, clinically associated, or having unknown frequency or minor allele frequency < 0.001) predicted to be deleterious by the Combined Annotation Dependent Depletion (CADD)[11] (score > 15.0) or Database for Nonsynonymous SNPs' Functional Predictions (dbNSFP) Support Vector Machine

(SVM)[12] (radial score > 0.0) algorithm were retained and prioritized on the basis of the functional relevance of genes using GeneDistiller. Genes were ranked based on combinations of terms from the OMIM clinical synopsis for MIM 601088 and 601353 (i.e., cataract, deafness, mental retardation, facial dysmorphism, short stature, and seizure) as keywords, using similarity of expression patterns and protein-protein interactions as major weights. We obtained the highest score for *MAF*, a gene whose mutations had previously been reported to cause autosomal dominant congenital cataracts and lens abnormalities (MIM 610202).[13,14] Sanger sequencing confirmed heterozygosity for the c.161C>T (p.Ser54Leu) change in the proband, and sequencing of parental DNAs revealed only the reference allele, evidence for its de novo origin (Figure S1). STR genotyping (AmpFlSTR Identifiler Plus [Life Technologies]) confirmed paternity. The variant was documented in the proband's skin fibroblasts as well as hair bulb and buccal epithelial cell specimens, strongly arguing against the possibility of a somatic event (Figure S1). All the other candidate variants turned out to be inherited from one of the unaffected parents (Table S4).

To confirm the causal involvement of *MAF*, we scanned the entire coding sequence of the gene (NM_005360.4 and NM_001031804.2) for mutations in DNA samples from 12 additional subjects (Table S1), including a sib pair, with features overlapping the conditions delineated by Gripp et al.[1] and Aymé and Philip,[2] by direct sequencing. Primer pairs designed to amplify the *MAF* coding exons and their intron boundaries (NC_000016.10, 79593848..79600725) are listed in Table S5. We identified heterozygous missense mutations in seven unrelated individuals (Table 1 and Figure S1). Two different changes affected Thr58 and Pro59, while others involved adjacent residues, including the previously identified c.161C>T substitution. In all family trios for which parental DNA samples were available, genotyping documented the de novo origin of each mutation, and STR analysis confirmed paternity (Table 1). Sanger sequencing of DNA from available oral mucosal epithelial cells (case 11-1), or epithelial cells and fibroblasts (case 4-1) supported the germline origin of mutations. All changes were predicted to impact protein function by dbNSFP and/or CADD (Table 1), and affected residues conserved among orthologs and paralogs (Figure S2).

MAF is a basic leucine zipper (bZIP)-containing transcription factor of the AP1 superfamily.[15,16] It is important for lens and eye development[17,18] and controls multiple physiological processes, including mechanosensory function, and chondrocyte and T cell differentiation.[19–21] Immunohistochemical analyses in mouse embryos documented wide *Maf* expression (Figure S3). Consistent with previous reports, we observed Maf staining in the lens, dorsal spinal cord, dorsal root ganglia, skin, kidney, hypertrophic chondrocytes of vertebrae, rib and limb cartilage, and the cartilage primordium of the basioccipital bone.[22,23] In line with the sensorineural hearing loss occurring in
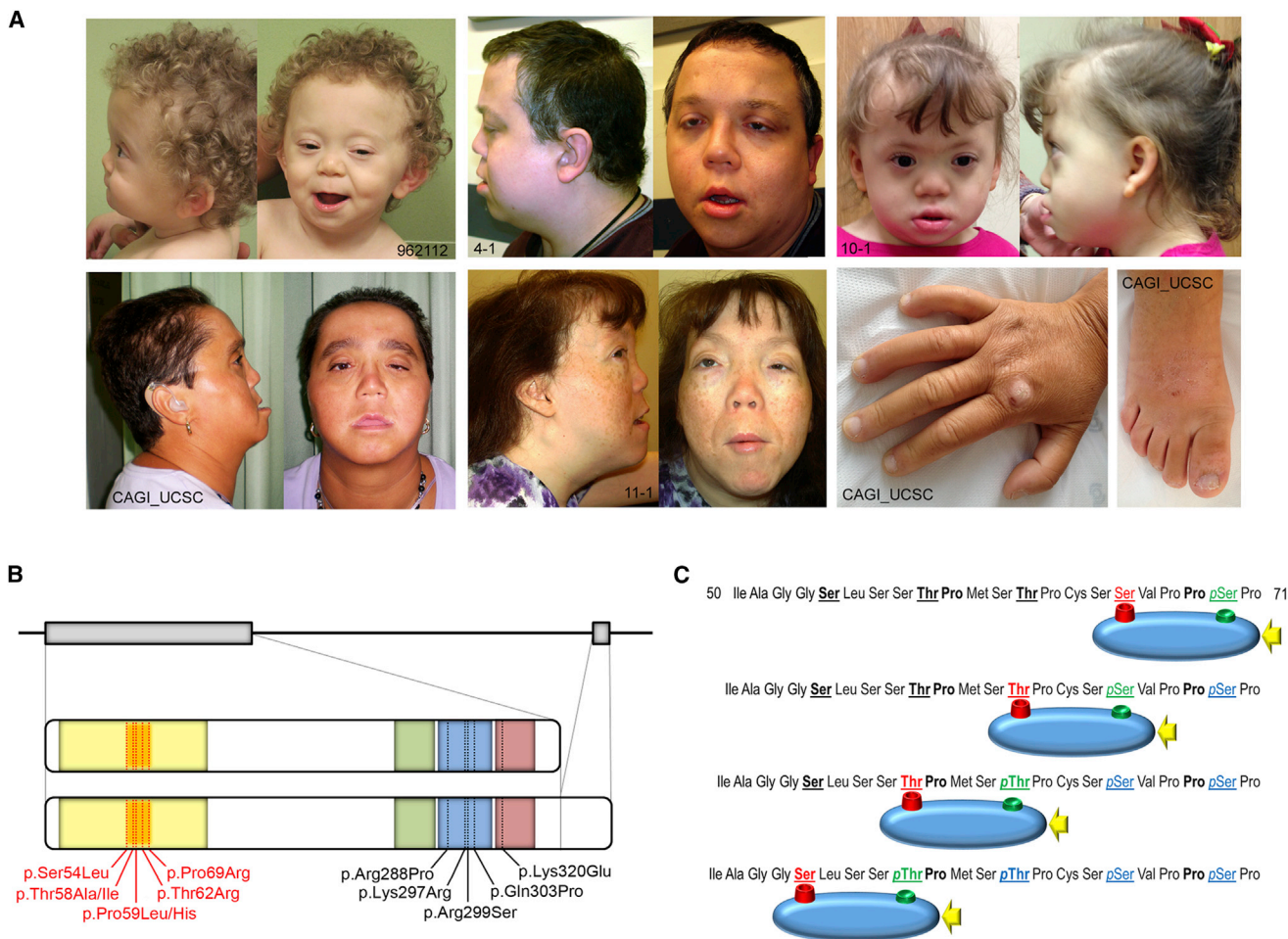
Figure 1. **De Novo Heterozygous Missense Mutations Affecting Residues of the GSK3 Phosphorylation Motifs within the Transactivation Domain of MAF Cause Aymé-Gripp Syndrome**

(A) Clinical features of affected subjects. Note the distinctive flat face, brachycephaly, ptosis, short nasal tip, long philtrum, small mouth, low-set and posteriorly angulated ears, and nail dystrophy. Permission to publish photographs was provided for all subjects shown.

(B) Scheme of the MAF domain structure, and location of *MAF* mutations causing human disease. MAF contains an N-terminal transactivation domain (yellow) with regulatory function, and a C-terminal DNA binding domain, the latter containing an "extended homology" (green), "basic motif" (light blue), and leucine-zipper (pink) regions. The region containing the four in tandem arranged phosphorylation sites recognized by GSK3 (orange) is located within the transactivation domain. Residues mutated in subjects with Aymé-Gripp syndrome (red) and previously reported isolated cataracts/eye defects (black) are shown.

(C) Cartoon illustrating the GSK3 recognition motifs and location of residues affected in Aymé-Gripp syndrome. The GSK3 catalytic domain is depicted with its active site (red) and the site binding to the priming phosphorylated residue (green). To phosphorylate its substrates, GSK3 requires a priming phosphorylation on the substrate four amino acids downstream the residue to be phosphorylated. The serine/threonine residues sequentially targeted by GSK3 are shown (red). Upon phosphorylation, they act as priming residues (green) to allow the subsequent phosphorylation of the upstream Ser/Thr. The kinase phosphorylating Ser70 has not been characterized yet. The residues affected by Aymé-Gripp syndrome-causing mutations (Ser54, Thr58, Pro59, Ser62, and Pro69) are indicated in bold.

all mutation-positive subjects, we detected a specific and strong signal in cochlear cells of E14.5 embryos.

Similar to other "large" MAF subfamily members (i.e., MAFA, MAFB, and NRL), MAF's structure is characterized by a C-terminal extended homology region and bZIP domain mediating DNA binding, and a N-terminal transactivation domain required for transcriptional activity and regulatory function (Figure 1B). The latter contains four GSK3 phosphorylation motifs, highly conserved among large MAF proteins (Figure 1C). In MAFA, the sequential phosphorylation of these serine/threonine residues promotes ubiquitination and rapid degradation, but also in-

creases transactivation potential.[24,25] Remarkably, all identified *MAF* mutations clustered within these motifs. Three affected residues, Ser54, Thr58, and Ser62, are known GSK3 phosphorylation target sites.[26] The remainder did not involve phosphorylatable residues, but were predicted to affect GSK3-mediated phosphorylation by altering proline residues adjacent to either a phosphorylation site (Thr58) or the C-terminal priming site (Ser70), whose phosphorylation is absolutely required for GSK3 function. To explore the impact of the p.Pro59His, p.Pro59Leu, and p.Pro69Arg changes, we performed molecular dynamics (MD) simulations on complexes formed by full-length

Table 1. *MAF* Mutations Identified in Individuals with Aymé-Gripp Syndrome

Subject	Reference	Nucleotide Change[a]	Amino Acid Change[a]	Protein Domain	Inheritance	Functional Impact (Radial SVM Score/ CADD Score)
1 (19474)	2	c.161C>T	p.Ser54Leu	TD	De novo	1.10/16.27
2 (11-1)	1	c.172A>G	p.Thr58Ala	TD	De novo, germline	0.83/16.07
3 (4-1)	1	c.206C>G	p.Pro69Arg	TD	De novo, germline	0.98/15.49
4 (ICN_ICW)	5	c.173C>T	p.Thr58Ile	TD	Not available[b]	0.93/15.38
5 (14-1)	4	c.176C>A	p.Pro59His	TD	De novo	1.10/17.69
5 (10-1)	p.s.	c.176C>T	p.Pro59Leu	TD	De novo	0.98/9.08
7 (962112)	p.s.	c.185C>G	p.Thr62Arg	TD	De novo	1.10/17.88
8 (CaGi_UCSC)	p.s.	c.161C>T	p.Ser54Leu	TD	De novo, germline	1.10/16.27

p.s., present study; TD, transactivation domain.
[a]Nucleotide and amino acid positions refer to transcript variant 1 and protein isoform a (longer isoform) (NM_005360.4, NP_005351.2).
[b]Parental DNAs were not available for molecular analyses.

GSK3 and ten residue-long peptides of MAF corresponding to the segment that interacts directly with the GSK3 binding cleft, encompassing both the GSK3 target and pSer/pThr primed residues (Table S6). The starting coordinates for the ATP-bound GSK3 were taken from the crystallographic structure of GSK3B complexed with AMP-PNP (PDB entry 1pyx).[27] Each decapeptide was set in an extended conformation along the catalytic cleft of GSK3 as specified in Table S6. The MD simulations were carried out according to the protocol previously described.[10] The Gromos 53a6 force field was used, with the exception of the partial charges of pSer/pThr,[28,29] and the parameters for ATP, obtained from quantum mechanical calculation of the molecular system reported in Figure S4. For p.Pro59-His and p.Pro59Leu decamers, the conformation of the trimer comprised between the substrate and primed residues was rearranged considerably during the simulations (Figure 2A and Figure S5), with the correct orientation of the substrate residue in the GSK3 active site being destabilized (Figure 2A). p.Pro69Arg, introducing a cationic residue in the proximity of the positively charged GSK3 priming pocket formed by residues Arg96, Arg180, and Lys205, caused a general rearrangement of the adjacent pSer70, pulling it away from the binding pocket (Figure 2B). Overall, our simulations indicated consistently that all disease-causing *MAF* mutations inhibit GSK3-mediated phosphorylation through impaired association and/or catalysis, by perturbing the interaction with the priming site (p.Pro69Arg) or the active site (substitutions affecting Pro59).

To explore the mutations' functional impact directly, we evaluated MAF phosphorylation status. The disease-causing p.Ser54Leu, p.Thr58Ala, p.Thr58Ile, p.Pro59Leu, p.Pro59His, and p.Pro69Arg (FLS-like disorder), and p.Arg288Pro (c.863G>C) changes, the latter considered as representative of lesions associated with isolated cataract,[13] were introduced into the *MAF* cDNA cloned in pCS2+ vector using the QuikChange Site-Directed Mutagenesis Kit (Agilent Technologies). Consistent with previous reports,[26] Western blot analysis of transiently transfected COS1 cell lysates documented two MAF states: a slower-migrating, fully phosphorylated form, and a faster-migrating, unphosphorylated form. In cells expressing wild-type *MAF*, the phosphorylated protein (upper band) predominated, while unphosphorylated MAF (lower band) was barely detectable (Figure 3A, upper panel). Similarly, the mutant carrying the p.Arg288Pro substitution in the DNA binding domain, previously associated with isolated lens and eye defects, was efficiently phosphorylated. This was in sharp contrast to all MAF mutants identified in the present study, which accumulated in cells as unphosphorylated proteins. GSK3-mediated phosphorylation represents a regulatory mechanism promoting MAFA ubiquitination and degradation.[24,25] Based on the high conservation of the GSK3 recognition motif and MAF being a GSK3 substrate, we hypothesized that the amino acid changes in our affected subjects might mediate inefficient protein clearance. On Western blot analyses, we noted increased protein levels (Figure 3A, upper panel) and decreased ubiquitination (Figure 3A, middle panel) for the disease-causing MAF mutants when compared to the wild-type protein (Figures 3A and 3B). Treatment with cycloheximide (CHX), a protein synthesis inhibitor, showed that the half-life of wild-type MAF was much shorter than that of the mutants (Figure 3B). Indeed, a complete disappearance of the protein was observed upon 4 hr CHX treatment, while the steady-state level of the mutants was largely unchanged. Consistently, treatment with MG132, which specifically inhibit proteasomal function, stabilized the protein level of wild-type MAF, while it did not have any significant effects on mutants (Figure 3B). Taken together, these results showed that mutations prevented MAF degradation and enhanced their stability. Of note, a partial phosphorylation was apparent for the p.Pro69Arg MAF mutant, which was associated with increased degradation via proteasome, even though less efficiently compared to wild-type MAF. This finding
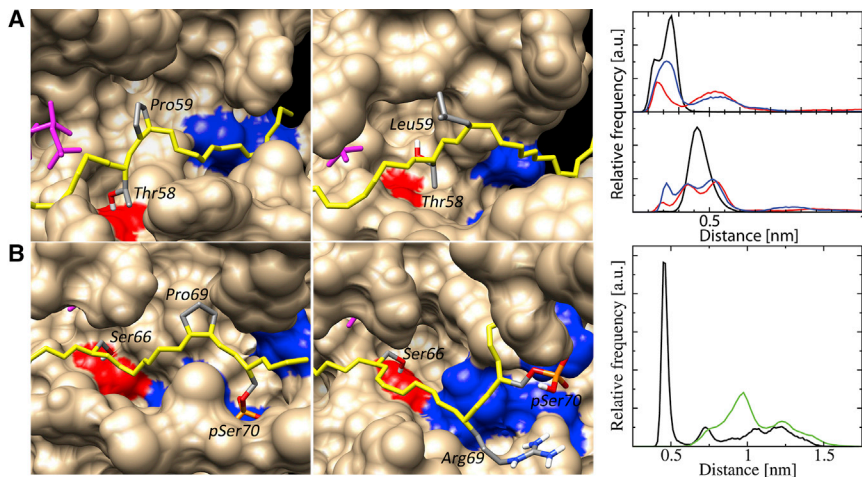
Figure 2. Molecular Dynamics Simulations of the GSK3/MAF Decapeptide Complexes

(A) Structural effects of the p.Pro59Leu and p.Pro59His changes. In both mutants, the conformation of the trimer comprised between the target and primed residues is considerably rearranged. Representative conformations are reported for wild-type MAF (left) and the p.Pro59Leu mutant (middle). In both mutants, larger and more variable distances are observed between the hydroxyl of Thr58, which is a GSK3 target residue, and the γ-phosphate of ATP (right, top plot) or the carboxyl group of the catalytic residue Asp181 (right, bottom plot). The distribution obtained in the simulations of the wild-type MAF sequence (black) and those referred to the peptides containing the p.Pro59His (red) and p.Pro59Leu (blue) substitutions are shown.

(B) Effect of the p.Pro69Arg change. In the simulations, a stable interaction between pSer70 of the wild-type peptide and the priming site was observed (left), while a displacement of that residue from the site was documented for the peptide carrying the p.Pro69Arg change (middle). Such structural rearrangements are quantified by the distance occurring between the P atom of pSer70 and the ω-carbon atom in the side chain of the GSK3 priming site residue, Arg180 (wild-type peptide, black; p.Pro69Arg peptide, green) (right). In the left and middle panels, the surface of GSK is colored in brown, except for the catalytic residue Asp181 (red), and the priming site residues, Arg96, Arg180, and Lys205 (blue). ATP is shown in pink and the MAF backbone in yellow. The side chains of priming, target, and mutated MAF residues are shown in sticks representation.

suggests a milder perturbing role of the proline-to-arginine substitution on GSK3-mediated phosphorylation at Ser66 compared to the other disease-causing amino acid changes, possibly due to the peculiar effect of the introduced arginine residue, which was documented to primarily affect MAF interaction with the GSK priming site. Confocal microscopy of transfected COS1 cells confirmed the nuclear localization of all tested mutants and their higher abundance within cells (Figure 3C). Moreover, treatment with CSK buffer prior fixation indicated that the syndrome-causing mutants retained efficient interaction with chromatin suggesting that they bind to DNA, in contrast to the DNA binding-impaired cataract-associated p.Arg288Pro mutant (Figure 3C and Table S7). Transactivation assays using luciferase as reporter under control of the IL4 promoter documented that COS1 cells transiently expressing the cataract-causing mutant allele had barely detectable reporter induction (Figure 3D). In contrast, cells expressing the p.Ser54Leu, p.Thr58Ala, p.Thr58Ile, p.Pro59Leu, p.Pro59His, or p.Pro69Arg MAF coding alleles showed efficient induction of luciferase levels, though not reaching the levels of the wild-type protein, suggesting that, despite their stabilization and much higher levels, these mutants are less active, at least under these specific conditions.

Next, we conducted gene-expression profiling analyses on primary skin fibroblasts from two unrelated subjects (4-1 and CaGi_UCSC) to explore more globally the impact of dysregulated MAF function on gene expression (Table S8 for details). Approximately 6% of genes in mutation-positive subject-derived cells were expressed differentially compared to control fibroblasts (ATCC code PCS-201-012). Gene ontology enrichment analysis of these differen-

tially expressed genes revealed an overrepresentation of genes coding for proteins associated with developmental programs (tissue morphogenesis, branching morphogenesis, urogenital system, and bone development) and cellular processes (cytoskeletal rearrangement, cell migration and adhesion, and response to extracellular stimuli) (Table S8). Publicly available microarray data (ArrayExpress accession code E-GEOD-51231) allowed selection of genes whose expression is positively controlled by MAF. Remarkably, these putative targets were observed to be enriched significantly in up- or downregulated transcripts in *MAF* mutation-positive fibroblasts (Figure S6), suggesting a complex, promoter-specific dominant dysregulatory function of these mutations.

Because cognitive deficits, with or without brain defects, are invariably present among subjects with *MAF* mutations affecting the GSK3 recognition motif, but absent in individuals with congenital cataracts caused by *MAF* mutations involving the DNA binding domain,[13,30–33] we posited that expression of the mutant alleles here identified should induce defects in neurogenesis, whereas alleles driving dominant cataracts through a haploinsufficiency model should not. To test this hypothesis in vivo, we analyzed the impact of these mutation classes on the integrity of the central nervous system (CNS) using a zebrafish model. The optic tectum is a major component of the vertebrate midbrain, comprising a structure equivalent to the mammalian superior colliculus, with external layers collecting sensory information and internal layers having a motor-function. We previously showed that measurement of the area of this structure represents a robust surrogate for brain volume and that reduction of the absolute area of the tectum
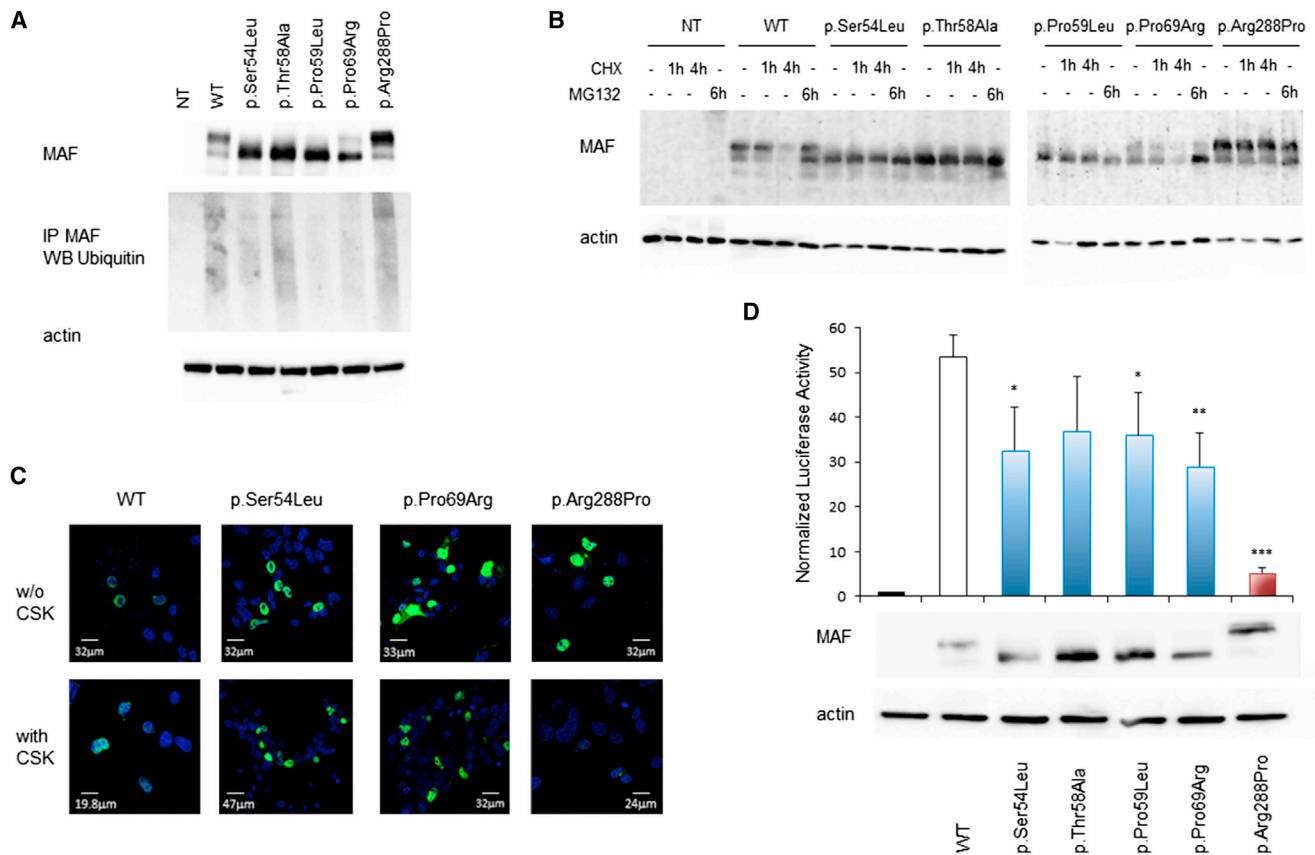
Figure 3. Impact of Disease-Causing Mutations on MAF Function

(A) Protein and phosphorylation levels of wild-type and disease-causing mutant MAF proteins in transiently transfected COS1 cells (upper panel). COS1 cells were maintained in high glucose DMEM, plus 10% FBS and supplements, and were transiently transfected to express wild-type *MAF* or each of the disease-causing alleles (FuGENE 6 [Promega]). To assess ubiquitination, we probed immunoprecipitated MAF with an anti-ubiquitin antibody (#8017, Santa Cruz Biotechnology) (middle panel). Whole-cell extracts were blotted with anti-MAF polyclonal (#7866, Santa Cruz Biotechnology), and anti-β-actin monoclonal (#A5441, Sigma-Aldrich) antibodies. Western blots are from a representative experiment of three performed.

(B) Protein stability and proteasome-dependent degradation were assessed in COS1 cells transfected with the indicated constructs. Twenty-four hours after transfection, cells were treated with 20 μg/ml cycloheximide (CHX) or 20 μM MG132 for the indicated times. MAF protein levels were detected by immunoblotting with anti-MAF antibody. Western blots of a representative experiment of three performed are shown.

(C) Confocal laser scanning microscopy analysis performed in COS1 cells transiently expressing wild-type *MAF* or one of three disease-causing alleles, without (upper panels) or with (lower panels) treatment with CSK buffer prior fixation. Cells were stained with anti-MAF polyclonal antibody and Alexa Fluor 488 goat anti-rabbit secondary antibody (green). Nuclei are DAPI stained (blue). Images are representative of 450 analyzed cells (Table S7). Experiments were performed as previously reported.[10]

(D) Transactivation assays were performed in COS1 cells transiently cotransfected with the *IL4* promoter cloned into pGL3 vector reporter construct (kindly provided by Michael Lohoff, University of Marburg, Marburg, Germany) alone (black bar) or together with wild-type MAF (white bar) or each of the disease-causing MAF mutants (blue and red bars) (1:1 ratio), and 1:10 of *Renilla* luciferase control vector DNA (pRL-Act *Renilla*). After transfection (24 hr), firefly and *Renilla* luciferase activities were measured by the Dual Luciferase Reporter Assay System (Promega). Normalized luciferase activity (mean ± SD) of six experiments performed is reported as fold increase relative to cells not expressing exogenous *MAF*. p values were calculated using two-tailed Student's t test. *, **, and *** indicate $p < 0.05$, $p < 0.01$, and $p < 0.001$, respectively. Protein levels of wild-type and disease-causing mutant MAF proteins were evaluated by immunoblotting with anti-MAF and anti-actin antibodies (lower panels).

correlates with neurodevelopmental defects in humans.[34,35] We injected clutches of 50–100 embryos with human mRNA encoding wild-type MAF, each of four alleles carrying mutations discovered in the present study, or the cataract-associated allele. Experimental work was carried out under protocols approved by the Institutional Animal Care and Use Committee of the Duke University, as previously described.[34–36] Following quantitative measurement of the surface area of the tecta (blind to injection cocktail; replicated), we observed that expression of either wild-type and cataract-associated (c.863G>C; p.Arg288Pro) *MAF* mRNAs did not induce appreciable brain volume differences. In contrast, injection of human *MAF* mRNA encoding each of the p.Ser54Leu, p.Thr58Ala, p.Pro59Leu, or p.Pro69Arg changes caused a statistically significant reduction of the size of the optic tecta ($p < 0.0001$; Figure 4). These data were concordant with our in vitro model and provided further evidence for the
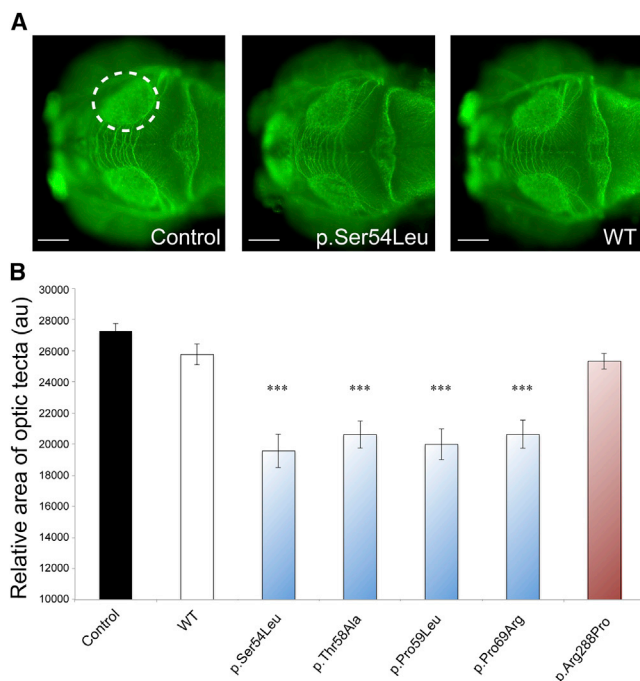
Figure 4. In Vivo Impact of Aymé-Gripp Syndrome- and Isolated Cataract-Causing *MAF* Mutations on the Integrity of the Central Nervous System Using a Zebrafish Model

(A) Dorsal views of uninjected zebrafish embryos (left), and embryos injected with the Aymé-Gripp syndrome-causing mutant (c.161C>T; p.Ser54Leu) (middle) and wild-type (right) *MAF* capped mRNA (100 pg) at 3 days after fertilization (dpf). Embryos were whole-mount stained using a primary antibody against acetylated tubulin (1:1000, T7451 [Sigma-Aldrich]) that marks neuronal axons, and an Alexa Fluor goat anti-mouse IgG secondary antibody (1:1000, A21207, Invitrogen). The circle highlights the area of the optic tectum that was measured.

(B) Overexpression of wild-type *MAF* or the congenital cataracts-causing (c.863G>C; p.Arg288Pro) allele do not induce a significant reduction in the size of the optic tectum. By contrast, overexpression of each of the Aymé-Gripp syndrome-causing alleles results in a statistically significantly reduction of the size of the optic tectum (p < 0.0001). Bars indicate SE, and AU denotes arbitrary units. Statistical analysis was performed using two-tailed Student's t test. For the measurements performed, we scored 86 control embryos, 61 embryos injected with wild-type *MAF* mRNA, and 58–70 embryos with each of the Aymé-Gripp syndrome-causing alleles' mRNA. All experiments were performed blind to injection cocktail in duplicate.

differential impact of these two mutation classes on CNS development.

Individuals with *MAF* mutations shared congenital or early onset cataracts, sensorineural hearing loss, developmental delay/intellectual disability, seizures, brachycephaly, midfacial hypoplasia, and reduced growth (final height −2.25 to −4 SD) as major characteristics (Figure 1A and Table S1). Bilateral hearing loss was diagnosed in early childhood and had at least a moderate to severe sensorineural component in all, in some cases requiring hearing aids. Limited information on inner ear imaging is available. Facial features were distinctive and recognizable, and included a short nasal tip and long philtrum, a small mouth, and small/low-set posteriorly

angulated ears. Late closing anterior fontanel, radio-ulnar synostosis or limited elbow movement occurred in several subjects, as did pericardial effusion and idiopathic chondrolysis of the hip. The three adult females had mammary gland hypoplasia, and two lacked axillary hair. Two individuals showed hypopigmented retinal lesions. Mesangiocapillary glomerulopathy occurred in the oldest affected individual. While intellectual function was not assessed systematically, impairment was universally present. Adaptive function in adult individuals ranged from severely autistic, nonverbal and requiring medication for behavior problems to working in a supervised community environment and living with guardians. Seizures and abnormal EEG findings consistent with focal and diffuse abnormal activity were present in all individuals, most often diagnosed in early childhood. Brain imaging studies commonly showed prominence of the axial and extra-axial fluid spaces; other anomalies like a Chiari 1 malformation or J-shaped sella occurred in single cases. The absence of mutations among subjects with only partly overlapping features (e.g., absence of brachycephaly and cataracts in sibs 10 and 11, and facies not suggestive in case 13) implies that mutations affecting residues within the GSK3 recognition motif of MAF cause a clinically homogeneous phenotype, and that cataracts, sensorineural hearing loss, intellectual disability, seizures, brachycephaly, Down syndrome-like facial appearance, and reduced growth are likely to represent cardinal features of the disorder.

Transcription factors operate in developmental processes to mediate inductive events and cell competence, and perturbation of their function or regulation can dramatically affect morphogenesis, organogenesis, and growth.[37] Here we establish that missense mutations impairing GSK3-mediated MAF phosphorylation severely perturb multiple developmental processes. Inactivating missense mutations affecting the MAF DNA binding domain had been reported to cause congenital cataracts, microcornea and iris coloboma.[13,30–33] Contrasting those mutations, we describe a class of missense changes not impairing DNA binding, but instead precluding post-translational modifications required for proteasomal degradation, resulting in mutants being more stable than wild-type MAF. In addition to defective degradation, this *MAF* mutation class showed perturbed in vitro transactivation activity, and endogenous expression in primary fibroblasts was associated with both up- and downregulation of genes identified as positively controlled MAF targets. These findings support the idea that, besides promoting degradation, GSK3-mediated MAF phosphorylation impacts protein activity through other mechanisms, as previously demonstrated for MAFA,[24] and suggest a complex pathogenetic mechanism involving protein stability and functional dysregulation. Of note, dominant missense mutations affecting residues in the same regulatory motif of MAFB and NRL, including those homologous to Ser54, Pro59, Thr62, and Pro69, have been reported to cause multicentric carpotarsal osteolysis (MCTO [MIM

166300]) and autosomal dominant retinitis pigmentosa (RP27 [MIM 613750]) (Figure S2), respectively,[38,39] further highlighting the critical role of this domain.

Early onset cataracts and hearing loss have rarely been reported in genetic conditions, with the collagenopathies, Alport (MIM 104200), Stickler (MIM 108300) and Marshall (MIM 154780) syndromes being the most common. This work identified *MAF* mutations as principal cause for a disorder combining cataracts and hearing loss in a multi-system developmental syndrome independently recognized by Gripp et al.[1] and Aymé and Philip.[2] Though the clinical presentation of subjects within this study resembles that described in the context of FLS, we note that this overlap is only partial. Moreover, FLS has been applied to clinically variable phenotypes of likely heterogeneous etiology (here exemplified by cases 10, 11, and 12). We therefore propose the eponym Aymé-Gripp syndrome for the disorder caused by mutations affecting residues of the GSK3 phosphorylation motifs in order to distinguish the phenotype described here from that reported by Fine and Lubinsky.[3]

By regulating the spatio-temporal expression of tissue-specific genes, MAF proteins act as key regulators of terminal differentiation in many tissues and organs, including bone, brain, kidney, lens, pancreas, and retina.[40,41] While apparently no gross anomalies are associated with Maf haploinsufficiency in mice, $Maf^{-/-}$ pups die soon after birth and exhibit defective lens formation and eye development,[17,18] chondrocyte terminal differentiation,[21] as well as differentiation and function of mechanoreceptors and neurons with mechanosensory function.[20,42] In contrast, a semi-dominant, missense mutation (c.881G>A, p.Arg291Gln) affecting the DNA-binding domain of Maf and causing a reduced transactivation activity of the transcription factor has been associated with congenital cataract in heterozygote mice,[14] recapitulating the hypomorphic cataracts-associated *MAF* mutations in humans.[13,30–33] Finally, a functionally distinct missense change (c.269A>T, p.Asp90Val) affecting the N-terminal transactivation domain and promoting enhanced transactivation function in Maf has been shown to cause a dominant isolated cataract phenotype.[43] Contrary to these loss-of-function, gain-of-function, and haploinsufficiency models, we here showed a distinct, dominantly acting effect of *MAF* mutations underlying a complex developmental disorder affecting multiple organs and tissues. As such, the pleiotropic effect of impaired MAF phosphorylation in Aymé-Gripp syndrome expands the perturbing consequences of dysregulated MAF function for multiple developmental programs, establishing its role in morphogenesis, CNS development, hearing and growth, and delineates a novel instance of protein dosage effect in human disease.

Accession Numbers

The ArrayExpress accession number for the microarray data generated in this paper is E-MTAB-3250, and the RefSNP numbers of the disease-causing mutations are rs727502766 (c.161C>T), rs727502767 (c.172A>G), rs727502768 (c.206C>G), rs727502769 (c.173C>T), rs727502770 (c.176C>A, c.176C>T), and rs727502771 (c.185C>G).

Supplemental Data

Supplemental data include six figures and eight tables and can be found with this article online at http://dx.doi.org/10.1016/j.ajhg. 2015.03.001.

Web Resources

The URLs for data presented herein are as follows:

ArrayExpress, http://www.ebi.ac.uk/arrayexpress/
Combined Annotation Dependent Depletion (CADD), http://cadd.gs.washington.edu/
dbNSFP v.2.0, https://sites.google.com/site/jpopgen/dbNSFP
GeneDistiller, http://www.genedistiller.org/
NCBI Gene, http://www.ncbi.nlm.nih.gov/gene
OMIM, http://www.omim.org/
RCSB Protein Data Bank, http://www.rcsb.org/pdb/home/home.do

References

1. Gripp, K.W., Nicholson, L., and Scott, C.I., Jr. (1996). Apparently new syndrome of congenital cataracts, sensorineural deafness, Down syndrome-like facial appearance, short stature, and mental retardation. Am. J. Med. Genet. 61, 382–386.
2. Aymé, S., and Philip, N. (1996). Fine-Lubinsky syndrome: a fourth patient with brachycephaly, deafness, cataract, microstomia and mental retardation. Clin. Dysmorphol. 5, 55–60.
3. Fine, B.A., and Lubinsky, M. (1983). Craniofacial and CNS anomalies with body asymmetry, severe retardation, and other malformations. J. Clin. Dysmorphol. 1, 6–9.
4. Aymé, S., and Philip, N. (1997). Apparently new syndrome of congenital cataracts, sensorineural deafness, Down syndrome-like facial appearance, short stature, and mental retardation. Am. J. Med. Genet. 70, 333–335.

5. Keppler-Noreuil, K., Welch, J., and Baker-Lange, K. (2007). Syndrome of congenital cataracts, sensorineural deafness, Down syndrome-like facial appearance, short stature, and mental retardation: two additional cases. Am. J. Med. Genet. A. *143A*, 2581–2587.

6. Nakane, T., Mizobe, N., Hayashibe, H., and Nakazawa, S. (2002). A variant of Fine-Lubinsky syndrome: a Japanese boy with profound deafness, cataracts, mental retardation, and brachycephaly without craniosynostosis. Clin. Dysmorphol. *11*, 195–198.

7. Holder, A.M., Graham, B.H., Lee, B., and Scott, D.A. (2007). Fine-Lubinsky syndrome: sibling pair suggests possible autosomal recessive inheritance. Am. J. Med. Genet. A. *143A*, 2576–2580.

8. Schoner, K., Bald, R., Fritz, B., and Rehder, H. (2008). Fetal manifestation of the Fine-Lubinsky syndrome. Brachycephaly, deafness, cataract, microstomia and mental retardation syndrome complicated by Pierre-Robin anomaly and polyhydramnios. Fetal Diagn. Ther. *23*, 228–232.

9. Corona-Rivera, J.R., López-Marure, E., García-Cruz, D., Romo-Huerta, C.O., Rea-Rosas, A., Orozco-Alatorre, L.G., and Ramírez-Valdivia, J.M. (2009). Further clinical delineation of Fine-Lubinsky syndrome. Am. J. Med. Genet. A. *149A*, 1070–1075.

10. Cordeddu, V., Redeker, B., Stellacci, E., Jongejan, A., Fragale, A., Bradley, T.E., Anselmi, M., Ciolfi, A., Cecchetti, S., Muto, V., et al. (2014). Mutations in ZBTB20 cause Primrose syndrome. Nat. Genet. *46*, 815–817.

11. Kircher, M., Witten, D.M., Jain, P., O'Roak, B.J., Cooper, G.M., and Shendure, J. (2014). A general framework for estimating the relative pathogenicity of human genetic variants. Nat. Genet. *46*, 310–315.

12. Liu, X., Jian, X., and Boerwinkle, E. (2013). dbNSFP v2.0: a database of human non-synonymous SNVs and their functional predictions and annotations. Hum. Mutat. *34*, E2393–E2402.

13. Jamieson, R.V., Perveen, R., Kerr, B., Carette, M., Yardley, J., Heon, E., Wirth, M.G., van Heyningen, V., Donnai, D., Munier, F., and Black, G.C. (2002). Domain disruption and mutation of the bZIP transcription factor, MAF, associated with cataract, ocular anterior segment dysgenesis and coloboma. Hum. Mol. Genet. *11*, 33–42.

14. Lyon, M.F., Jamieson, R.V., Perveen, R., Glenister, P.H., Griffiths, R., Boyd, Y., Glimcher, L.H., Favor, J., Munier, F.L., and Black, G.C. (2003). A dominant mutation within the DNA-binding domain of the bZIP transcription factor Maf causes murine cataract and results in selective alteration in DNA binding. Hum. Mol. Genet. *12*, 585–594.

15. Blank, V., and Andrews, N.C. (1997). The Maf transcription factors: regulators of differentiation. Trends Biochem. Sci. *22*, 437–441.

16. Eychène, A., Rocques, N., and Pouponnot, C. (2008). A new *MAF*ia in cancer. Nat. Rev. Cancer *8*, 683–693.

17. Kim, J.I., Li, T., Ho, I.-C., Grusby, M.J., and Glimcher, L.H. (1999). Requirement for the c-Maf transcription factor in crystallin gene regulation and lens development. Proc. Natl. Acad. Sci. USA *96*, 3781–3785.

18. Ring, B.Z., Cordes, S.P., Overbeek, P.A., and Barsh, G.S. (2000). Regulation of mouse lens fiber cell development and differentiation by the *Maf* gene. Development *127*, 307–317.

19. Ho, I.C., Lo, D., and Glimcher, L.H. (1998). c-maf promotes T helper cell type 2 (Th2) and attenuates Th1 differentiation by both interleukin 4-dependent and -independent mechanisms. J. Exp. Med. *188*, 1859–1866.

20. Wende, H., Lechner, S.G., Cheret, C., Bourane, S., Kolanczyk, M.E., Pattyn, A., Reuter, K., Munier, F.L., Carroll, P., Lewin, G.R., and Birchmeier, C. (2012). The transcription factor c-Maf controls touch receptor development and function. Science *335*, 1373–1376.

21. MacLean, H.E., Kim, J.I., Glimcher, M.J., Wang, J., Kronenberg, H.M., and Glimcher, L.H. (2003). Absence of transcription factor c-maf causes abnormal terminal differentiation of hypertrophic chondrocytes during endochondral bone development. Dev. Biol. *262*, 51–63.

22. Sakai, M., Imaki, J., Yoshida, K., Ogata, A., Matsushima-Hibaya, Y., Kuboki, Y., Nishizawa, M., and Nishi, S. (1997). Rat maf related genes: specific expression in chondrocytes, lens and spinal cord. Oncogene *14*, 745–750.

23. Ogata, A., Shimizu, T., Abe, R., Shimizu, H., and Sakai, M. (2004). Expression of c-maf and mafB genes in the skin during rat embryonic development. Acta Histochem. *106*, 65–67.

24. Rocques, N., Abou Zeid, N., Sii-Felice, K., Lecoin, L., Felder-Schmittbuhl, M.P., Eychène, A., and Pouponnot, C. (2007). GSK-3-mediated phosphorylation enhances Maf-transforming activity. Mol. Cell *28*, 584–597.

25. Han, S.I., Aramata, S., Yasuda, K., and Kataoka, K. (2007). MafA stability in pancreatic beta cells is regulated by glucose and is dependent on its constitutive phosphorylation at multiple sites by glycogen synthase kinase 3. Mol. Cell. Biol. *27*, 6593–6605.

26. Herath, N.I., Rocques, N., Garancher, A., Eychène, A., and Pouponnot, C. (2014). GSK3-mediated MAF phosphorylation in multiple myeloma as a potential therapeutic target. Blood Cancer J *4*, e175.

27. Bertrand, J.A., Thieffine, S., Vulpetti, A., Cristiani, C., Valsasina, B., Knapp, S., Kalisz, H.M., and Flocco, M. (2003). Structural characterization of the GSK-3beta active site using selective and non-selective ATP-mimetic inhibitors. J. Mol. Biol. *333*, 393–407.

28. Oostenbrink, C., Villa, A., Mark, A.E., and van Gunsteren, W.F. (2004). A biomolecular force field based on the free enthalpy of hydration and solvation: the GROMOS force-field parameter sets 53A5 and 53A6. J. Comput. Chem. *25*, 1656–1676.

29. Hansson, T., Nordlund, P., and Aqvist, J. (1997). Energetics of nucleophile activation in a protein tyrosine phosphatase. J. Mol. Biol. *265*, 118–127.

30. Vanita, V., Singh, D., Robinson, P.N., Sperling, K., and Singh, J.R. (2006). A novel mutation in the DNA-binding domain of MAF at 16q23.1 associated with autosomal dominant "cerulean cataract" in an Indian family. Am. J. Med. Genet. A. *140*, 558–566.

31. Hansen, L., Eiberg, H., and Rosenberg, T. (2007). Novel MAF mutation in a family with congenital cataract-microcornea syndrome. Mol. Vis. *13*, 2019–2022.

32. Hansen, L., Mikkelsen, A., Nürnberg, P., Nürnberg, G., Anjum, I., Eiberg, H., and Rosenberg, T. (2009). Comprehensive mutational screening in a cohort of Danish families with hereditary congenital cataract. Invest. Ophthalmol. Vis. Sci. *50*, 3291–3303.

33. Narumi, Y., Nishina, S., Tokimitsu, M., Aoki, Y., Kosaki, R., Wakui, K., Azuma, N., Murata, T., Takada, F., Fukushima, Y., and Kosho, T. (2014). Identification of a novel missense mutation of MAF in a Japanese family with congenital cataract

by whole exome sequencing: a clinical report and review of literature. Am. J. Med. Genet. A. *164A*, 1272–1276.

34. Schulte, E.C., Kousi, M., Tan, P.L., Tilch, E., Knauf, F., Lichtner, P., Trenkwalder, C., Högl, B., Frauscher, B., Berger, K., et al. (2014). Targeted resequencing and systematic in vivo functional testing identifies rare variants in MEIS1 as significant contributors to restless legs syndrome. Am. J. Hum. Genet. *95*, 85–95.

35. Borck, G., Hög, F., Dentici, M.L., Tan, P.L., Sowada, N., Medeira, A., Gueneau, L., Thiele, H., Kousi, M., Lepri, F., et al. (2015). BRF1 mutations alter RNA polymerase III-dependent transcription and cause neurodevelopmental anomalies. Genome Res. *25*, 155–166.

36. Margolin, D.H., Kousi, M., Chan, Y.M., Lim, E.T., Schmahmann, J.D., Hadjivassiliou, M., Hall, J.E., Adam, I., Dwyer, A., Plummer, L., et al. (2013). Ataxia, dementia, and hypogonadotropism caused by disordered ubiquitination. N. Engl. J. Med. *368*, 1992–2003.

37. Gilbert, S.F. (2008). Principles of differentiation and morphogenesis. In Inborn errors of development. The molecular basis of clinical disorders of morphogenesis, Second edition, C.J. Epstein, R.P. Erickson, and A. Wynshaw-Boris, eds. (Oxford, New York: Oxford University Press), pp. 9–24.

38. Zankl, A., Duncan, E.L., Leo, P.J., Clark, G.R., Glazov, E.A., Addor, M.C., Herlin, T., Kim, C.A., Leheup, B.P., McGill, J.,

et al. (2012). Multicentric carpotarsal osteolysis is caused by mutations clustering in the amino-terminal transcriptional activation domain of MAFB. Am. J. Hum. Genet. *90*, 494–501.

39. Bessant, D.A.R., Payne, A.M., Mitton, K.P., Wang, Q.L., Swain, P.K., Plant, C., Bird, A.C., Zack, D.J., Swaroop, A., and Bhattacharya, S.S. (1999). A mutation in NRL is associated with autosomal dominant retinitis pigmentosa. Nat. Genet. *21*, 355–356.

40. Kataoka, K. (2007). Multiple mechanisms and functions of maf transcription factors in the regulation of tissue-specific genes. J. Biochem. *141*, 775–781.

41. Yang, Y., and Cvekl, A. (2007). Large Maf transcription factors: cousins of AP-1 proteins and important regulators of cellular differentiation. Einstein J. Biol. Med. *23*, 2–11.

42. Hu, J., Huang, T., Li, T., Guo, Z., and Cheng, L. (2012). c-Maf is required for the development of dorsal horn laminae III/IV neurons and mechanoreceptive DRG axon projections. J. Neurosci. *32*, 5362–5373.

43. Perveen, R., Favor, J., Jamieson, R.V., Ray, D.W., and Black, G.C. (2007). A heterozygous c-Maf transactivation domain mutation causes congenital cataract and enhances target gene activation. Hum. Mol. Genet. *16*, 1030–1038.